

Theoretical spectra and polarization in neutral-weak-boson production*

Leon B. Gordon[†] and R. W. Brown[†]

Institute for Theoretical Physics, State University of New York at Stony Brook, Stony Brook, New York 11794

(Received 12 May 1975)

We discuss the details of the theoretical predictions for the reaction $l^\pm + N \rightarrow Z^0 + l^\pm + N'$, in which the neutral weak vector boson is radiated by the lepton during electromagnetic recoil off of some nucleus. Energy and angular spectra for the boson, prompt lepton, recoiling proton, and decay leptons are considered. This agenda includes beam polarization effects and a study of the Z^0 polarization. Reference to previous charged-boson theoretical results simplifies our presentation considerably. Ancillary calculations for a scalar Z^0 possibility are described as well.

I. INTRODUCTION

An important component in the frenzied particle-search activity we see around us these days is interest in the hypothetical neutral intermediate weak boson Z^0 . This, of course, stems from recent experiments¹ in which weak neutral current effects have been observed, from the theoretical advantages of gauge theories,² and from the $J(\psi)$ phenomena (although it now appears that these new particles have nothing to do with the weak bosons).

Indirect propagator effects aside, the proof that this elusive particle exists lies ultimately in a specific production process. Over a decade ago, people^{3,4} thought about colliding electron beams as producers, an idea which has had its gauge-theory updating.⁵ The problem here, besides present limitations on beam energy, is the narrowness of the resonance enhancement. About this we need not elaborate but simply refer the reader to the discussion about the circumstances under which the new narrow resonances were found at SPEAR.⁶

The independent Brookhaven National Laboratory (BNL) discovery⁷ involving proton-proton collisions and electron-pair detection had the advantage of a variable lepton-pair "arm," an asset in looking for new particles. Even earlier, Ting had called the attention of Jaffe and Primack⁸ to this fact, who proceeded to estimate the cross sections for the production of charged and neutral weak bosons in inelastic proton-proton scattering. These estimates require a parton model and knowledge about quark couplings.

In a recent letter,⁹ we have considered an alternate reaction for study involving leptoproduction,

$$l^\pm + N \rightarrow l^\pm + N' + Z^0. \quad (i)$$

This process, given in lowest order by the diagrams in Fig. 1, has several advantages. Ignoring the amplitude of Fig. 1(c) for the moment, emission from a lepton line avoids hard questions about

hadron structure. The electromagnetic recoil off of some target N is described completely by the experimentally known form factors. Moreover, well above threshold the reaction can be coherent and a significant increase in the cross section obtains when the target is a heavy nucleus. As in proton-proton searches, one hopes to control backgrounds (from pions and their decays, for example) by the stipulation that large transverse momenta should be seen in the Z^0 decay products. We have the additional advantages of (a) having a good idea about the energy and angular spectra of the prompt (and decay) leptons and recoiling tar-

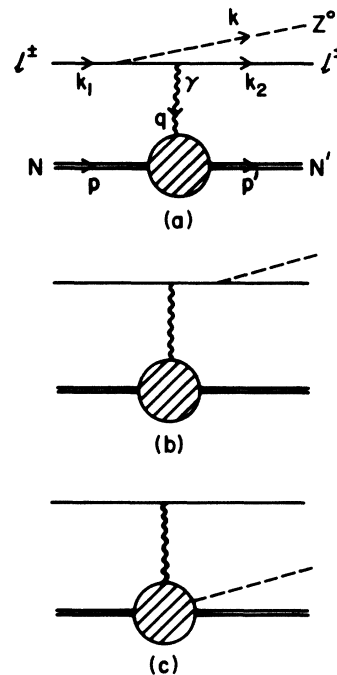


FIG. 1. Feynman diagrams and momentum assignments for the production of a weak neutral boson by the collision of charged leptons with a nuclear target.

get, and (b) knowing the reaction to be quasielastic so that production events should have few accompanying hadrons. The details of such an advantaged signature is the subject of this paper.

But what about hadron emission as depicted in Fig. 1(c)? The quasielastic channels may be suppressed by some combination of electromagnetic and weak form factors¹⁰ and a naive Boltzmann-factor argument with pion temperature¹¹ indicates that the (very) inelastic channels will not be important. On the other hand, one may get quite different conclusions from diffractive and parton pictures for the former and the latter channels, respectively. Some estimates of these mechanisms are in progress now¹² along with detailed consideration of the reaction¹³

$$\nu + N \rightarrow \nu + N' + Z^0. \quad (\text{ii})$$

The possibility in (i) of an electromagnetic interaction for the Z^0 (anomalous dipole and/or quadrupole moments) seems unimportant,¹⁴ but is also being considered in more detail.¹² As far as this paper is concerned, we shall stick to Figs. 1(a) and 1(b) and shall expect that the rates will simply increase when hadron emission is added in.

The specific motivation for Reaction (i) derives from the high-energy muon beams at the Fermi National Accelerator Laboratory (Fermilab). Early planning for Fermilab leaned towards muon beams for *charged* boson searches until it was seen that muon reactions were dynamically suppressed compared with neutrino reactions in spite of the higher muon beam energy (cf. discussion in Ref. 9). But this dynamical suppression is absent in *neutral* boson searches and, with the additional fact that (ii) has a marked absence of electric charges and correspondingly reduced rates, (i) is quite attractive. The reader should also keep in mind the future possibility of performing such an experiment with electron-proton colliding beams.¹⁵

The plan of this paper is as follows: Sec. II presents the calculation of the muon and boson differential cross sections, while Sec. III contains the spectra of the recoil proton. Two appendices are used for some of the detailed formulas of these two sections. We discuss polarization in Sec. IV and what happens if the Z^0 is a scalar boson in Sec. V. The dilepton decay distribution for the specific decay $Z^0 \rightarrow l^+ l^-$ can be found in Sec. VI. Some final remarks comprise Sec. VII.

II. MUON AND BOSON SPECTRA

For the weak part of the interaction Lagrangian, we take

$$\mathcal{L}_I = -\bar{\psi}\gamma_\mu(g_V - g_A\gamma_5)\psi Z^{0\mu}, \quad (2.1)$$

with

$$\frac{g_V^2 + g_A^2}{2} = \frac{M_Z^2 G_F^2}{\sqrt{2}}.$$

In the numerical results that follow, we will assume that the neutral coupling G_F is just the usual Fermi coupling, $G_F \approx 10^{-5}/m_p^2$. Neglecting hadronic emission, consideration of the lowest-order matrix element for the process (1.1) requires the evaluation of the two diagrams, Figs. 1(a) and 1(b).

Our notation is that of the figure with the four-vectors as shown.¹⁶ In particular, k_1 and k_2 refer to the initial and final lepton, respectively, while k refers to the Z^0 . We define

$$\begin{aligned} q &\equiv p' - p, \\ T &\equiv q^2, \\ S &\equiv (k_1 + p)^2, \end{aligned} \quad (2.2)$$

and we will consider a proton target at rest in the lab:

$$p = (M_p, \vec{0}). \quad (2.3)$$

Now, we may write down the expression for the differential cross section:

$$\begin{aligned} d^3\sigma &= \frac{1}{|\vec{v}_1|} \frac{\alpha^2}{128\pi^3 E_1 E_p} \delta^4(k_1 - k_2 - q - k) \\ &\times \frac{\mathcal{F}}{T^2} \frac{\mathcal{F}^2 k_2}{E_2} \frac{\mathcal{F}^2 k}{E_Z} \frac{\mathcal{F}^2 p'}{E_{p'}}, \end{aligned} \quad (2.4)$$

where

$$\mathcal{F} = K_{\alpha\beta} P_{\mu\rho} L^{\alpha\beta\mu\rho}.$$

Here, $K_{\alpha\beta} = \epsilon_\alpha^*(a)\epsilon_\beta(a)$ for a Z^0 of polarization $\epsilon_\alpha(a)$. In this section we will sum over polarizations, and

$$\sum_{\text{spin}} K_{\alpha\beta} = -g_{\alpha\beta} + \frac{k_\alpha k_\beta}{M_Z^2}. \quad (2.5)$$

The proton part of the matrix element is

$$P_{\nu\sigma} \equiv \frac{1}{2} \text{tr}\{(\not{p} + m_p)\bar{\Gamma}_\nu(\not{p}' + m_p)\Gamma_\sigma\}. \quad (2.6)$$

For a single proton, we can use the dipole fit to the form factors to write

$$P_{\nu\sigma} = (Tg_{\nu\sigma} - q_\nu q_\sigma)G_m^2 + P_\nu P_\sigma \frac{G_E^2 + \tau G_M^2}{1 + \tau}$$

with

$$\tau = \frac{-T}{4M_p^2}, \quad P = p + p', \quad (2.7)$$

$$G_E \approx \frac{G_M}{2.79} \approx \left[1 - \frac{T}{0.71 \text{ GeV}^2/c^2}\right]^{-2}.$$

Finally, the lepton part is given by

$$L^{\alpha\beta\mu\rho} = \text{tr} \left\{ (k_1 + \mu) \left[\frac{\gamma^\alpha (g_V - g_A \gamma_5) (2k_2^\mu + \not{q} \gamma^\mu)}{T_2} + \frac{(2k_1^\mu - \gamma^\mu \not{q}) \gamma^\alpha (g_V - g_A \gamma_5)}{T_1} \right] \right. \\ \left. \times (k_2 + \mu) \left[\frac{\gamma^\beta (g_V - g_A \gamma_5) (2k_1^\rho - \not{q} \gamma^\rho)}{T_1} + \frac{(2k_2^\rho + \gamma^\rho \not{q}) \gamma^\beta (g_V - g_A \gamma_5)}{T_2} \right] \right\}. \quad (2.8)$$

T and T_2 are the propagator denominators:

$$T_1 = (k_1 - q)^2 - \mu^2, \\ T_2 = (k_2 + q)^2 - \mu^2. \quad (2.9)$$

We can use current conservation to great advantage in doing this calculation by noting that $q_\mu L^{\alpha\beta\mu\rho} = 0$, and that $k_\alpha L^{\alpha\beta\mu\rho}$ would also be zero if we had a pure g_V interaction. The presence of the g_A term breaks the gauge symmetry, but only if $\mu \neq 0$ ¹⁷; in fact we see that the term $(k_\alpha k_\beta / M_Z^2) L^{\alpha\beta\mu\rho} \propto \mu^2 / M_Z^2$, and can be neglected to a good approximation.¹⁸ This makes the trace simple enough to be easily computed by hand.

We shall not labor the details of the phase-space integration here, except to remark that five of the integrations in (2.4) may be done trivially (the δ function and an over-all azimuthal angle), while the remaining four are done numerically. The details of the numerical integration are essentially the same as in the analogous charged boson calculations.¹⁹ Some further comments on this will be made in Appendix A.

The results of these calculations may be seen in Table I, and Figs. 2–5. The angular and energy distributions (which are independent of normalization) are essentially the same as in I and II; explanation of the qualitative features may be found there. The angular spectrum of the Z^0 (Fig. 2) shows very sharp forward peaking—for example, at $M_Z = 5 \text{ GeV}/c^2$ and $E_1 = 50 \text{ GeV}$, more than 95% of the cross section appears in the region $\cos\theta_Z$

> 0.999. The lepton distribution (Fig. 3) is also peaked in the forward direction, though not so sharply, with 83% of the cross section (at $M_Z = 5 \text{ GeV}/c^2$, $E_1 = 50 \text{ GeV}$) in the region $\cos\theta_l > 0.9$. Concomitant with the angular behavior is the observation that on the average, the Z^0 takes more than 90% of the available energy, while the prompt lepton obtains about 8%. Other details of the energy distributions are shown in Figs. 4–5. By the way, we might mention that to a very good approximation, the coupling in Eq. (2.1) results in just a factor of $(g_V^2 + g_A^2)$ multiplying the rest of the expression, so conversion to other couplings is immediate.²⁰

Noting that in the *extreme* high-energy limit, the Weizsäcker-Williams approximation²¹ for the total cross section yields

$$\sigma \underset{s \rightarrow \infty}{\approx} \frac{\alpha^2 G_F}{24\pi\sqrt{2}} \ln^3 \frac{2\kappa E}{M_Z^2}, \quad (2.10)$$

with κ a momentum-transfer cutoff, one could consider an expansion for the cross section of the form:

$$\sigma = \frac{\alpha^2 G_F}{24\pi\sqrt{2}} \ln^3 \frac{2\kappa E}{M_Z^2} + A \ln^2 \frac{2\kappa E}{M_Z^2} + B \ln \frac{2\kappa E}{M_Z^2} + C. \quad (2.11)$$

Unfortunately, the coefficients A, B, C are difficult to determine analytically and their dependence on M_Z makes a numerical fitting program of limited

TABLE I. Total cross sections for $l + p \rightarrow p + Z^0 + l$ in units of femtobarns ($1 \text{ fb} = 10^{-39} \text{ cm}^2$).

E_1 (GeV)	M_Z (GeV/ c^2)	3	5	8	10	15	20	25	30
50		109	14.2	0.00557	X	X	X	X	X
100		261	82.7	7.65	0.472	X	X	X	X
150		380	158	32.0	7.49	0.378×10^{-3}	X	X	X
200		477	228	63.9	22.6	0.213	X	X	X
250		558	291	98.4	42.4	1.77	0.444×10^{-4}	X	X
300		628	349	133	64.7	5.50	0.0223	X	X
400		744	450	201	112	18.8	0.954	0.356×10^{-3}	X
800		1040	737	427	293	105	31.2	5.92	0.407
1000		1150	840	517	371	153	56.2	16.2	2.79

use. We further mention that these coefficients are larger than the leading coefficient, so we cannot use the result (2.10) as a reasonable approximation.

III. PROTON SPECTRA

The proton differential cross sections, useful in target recoil studies, are most easily obtained by using a different technique than that of Sec. II. The method is based on the facts (a) that $P_{\mu\nu}$ (Eq. 2.6) depends only on the nucleon variables, and can be taken through the k and k_2 integrations, and (b) that the quantity

$$L^{\mu\nu} \equiv \int \frac{d^3 k_2}{E_2} \frac{d^3 k}{E_Z} \delta^4(k_1 - q - k_2 - k) \sum_{\text{spin}} K_{\alpha\beta} L^{\alpha\beta\mu\nu} \quad (3.1)$$

is a Lorentz tensor satisfying the conservation laws:

$$q_\mu L^{\mu\nu} = q_\nu L^{\mu\nu} = 0. \quad (3.2)$$

We thus have the usual Cottingham form²²

$$L^{\mu\nu}(k_1, q) = (g^{\mu\nu} q^2 - q^\mu q^\nu) t_1(k_1, q) + [q^2 k_1^\mu k_1^\nu - k \cdot q (k_1^\mu q^\nu + q^\mu k_1^\nu) + (k_1 \cdot q)^2 g^{\mu\nu}] t_2(k_1, q). \quad (3.3)$$

The symmetry of $P_{\mu\nu}$ allows us to ignore the possibility of pseudotensors in $L^{\mu\nu}$. We may now calculate the functions t_1 and t_2 in terms of the two quantities

$$L \equiv g_{\mu\nu} L^{\mu\nu}, \quad (3.4)$$

$$K \equiv k_{1\mu} k_{1\nu} L^{\mu\nu}.$$

L and K are most easily found by going to the lepton-boson center-of-mass frame in which the integrations in (3.1) can be done analytically. The result is that we need perform only the last two integrations numerically to determine

$$\sigma = \frac{1}{64\pi^2} \frac{\alpha^2}{|k_1| M_p} \int |\vec{p}'| dE_p d\cos\theta_p \frac{P_{\mu\nu} L^{\mu\nu}}{T^2}. \quad (3.5)$$

Some details of the calculation and the integration limits are given in Appendix B.

Results for the double differential cross section

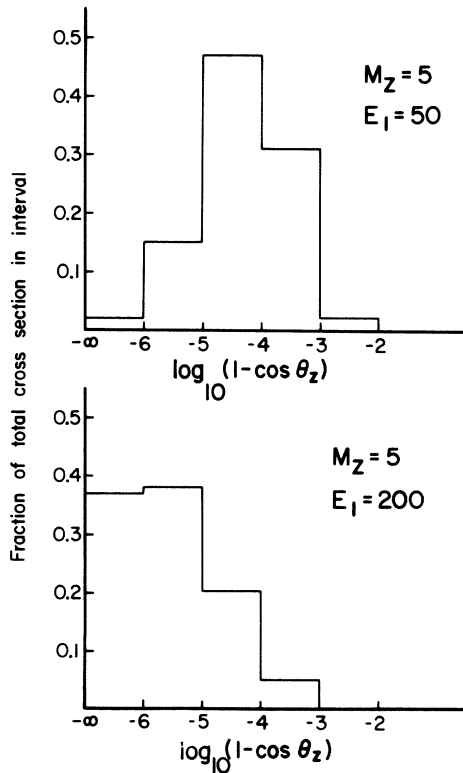


FIG. 2. Histograms of the fraction of the cross section per $\cos\theta_z$ interval for free proton targets. Here, $M_Z = 5 \text{ GeV}/c^2$ and $E_1 = 50$ and 200 GeV .

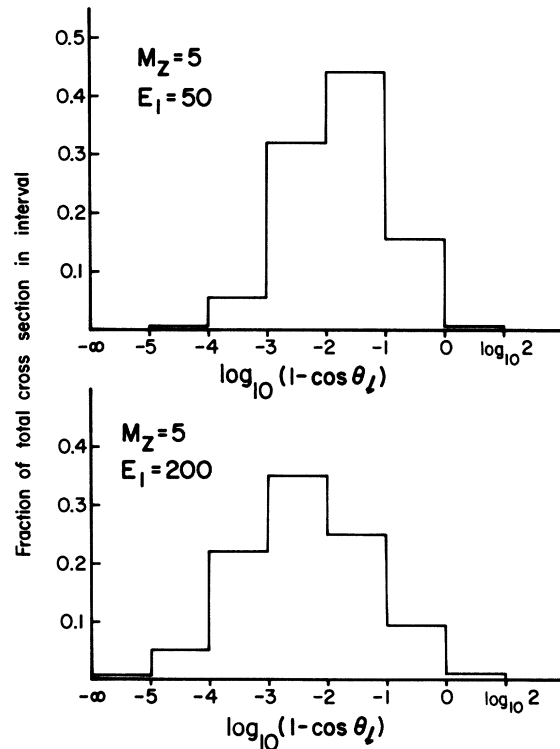


FIG. 3. Histograms of the fraction of the cross section per $\cos\theta_l$ interval for free proton targets. The boson mass and beam energy are as in Fig. 2.

of the recoil proton are exhibited in binned form in Fig. 6. The proton typically obtains little of the energy (~1-2%) and is scattered at a wide angle. Completing the integrations indicated in Eq. (3.5) yields a value for the total cross section which may be used as an independent check of the results given in Sec. II. The calculations compare well (differences are on the 1-2% level).

IV. POLARIZATION EFFECTS

There are two points to be considered here; first, the dependence of the cross section on the polarization of the beam, and second, the observed polarization of the emitted Z^0 .

With regard to the first, we note that in the high-energy limit with an unpolarized beam, the $(g_V - g_A \gamma_5)$ factors in Eq. (2.8) just yield an over-all factor $(g_V^2 + g_A^2)$ multiplying the total cross section. Suppose instead that we have a polarized l^+ beam of helicity λ :

$$\lambda = \begin{cases} -1 & \text{left-handed } l^+ \\ +1 & \text{right-handed } l^+ \end{cases}$$

Then the $(g_V^2 + g_A^2)$ factor is converted into

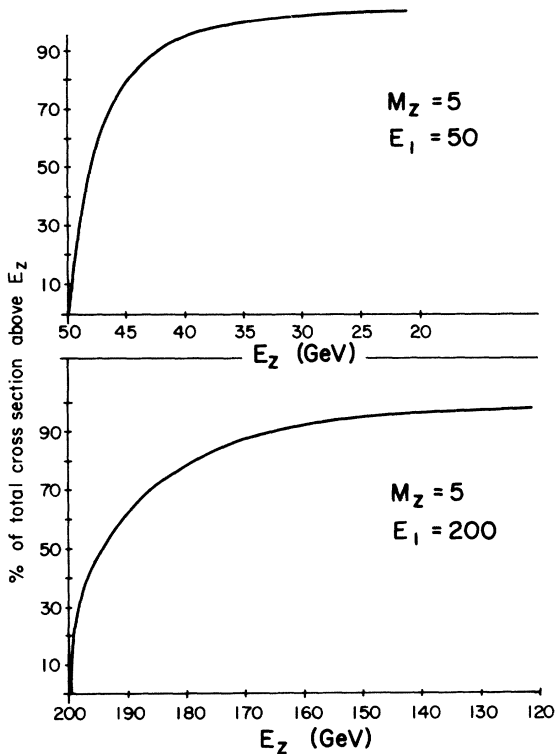


FIG. 4. Plot of the percentage of weak bosons with energy greater than a specific energy E_z for free proton targets. The boson mass and beam mass and beam energy are as in Fig. 2.

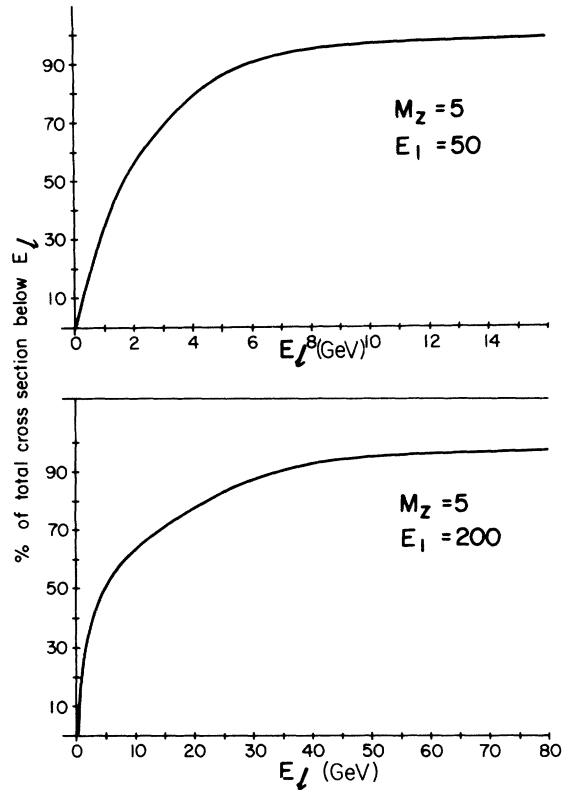


FIG. 5. Plot of the percentage of prompt leptons with energy less than a specific energy E_l for free proton targets. The boson mass and beam energy are as in Fig. 2.

$M_z = 5$
 $E_l = 50$

36.27	.006	.037	.021	0	0
4.56	.087	.86	6.7	.98	0
1.34	.248	2.13	25.4	49.8	0
1.02	.021	.26	3.44	10.1	0
.9921	0	.001	.013	0	0
.9380	1.	.999	.99	.9	.6
					$\cos \theta_p$

FIG. 6. Double binning for the recoil proton energy E_p and angle θ_p in percentage of cross section.

$\frac{1}{2}(g_V^2 + g_A^2 + 2g_V g_A^\lambda)$. The corresponding relation for an l^- beam is the same, but now

$$\lambda = \begin{cases} +1 & \text{left-handed } l^- \\ -1 & \text{right-handed } l^- \end{cases}$$

The implications for studying the relative sign of g_V and g_A are obvious.

The proper tool for studying the degree of polarization of the Z^0 is the density matrix.²³ We define the average density matrix as

$$\bar{\rho}_{ab} = \frac{1}{\sigma_{\text{tot}}} \sigma(\epsilon_\mu^*(a)\epsilon_\nu(b)). \quad (4.1)$$

That is, in computing the density matrix we use $K_{\alpha\beta} \equiv \epsilon_\alpha^*(a)\epsilon_\beta(b)$ directly rather than the sum in Eq. (2.5). The traces in this computation become rather long, so this work was performed with the aid of Veltman's algebraic computer program, SCHOONSCHIP.²⁴ Choosing the basis

$$\begin{aligned} \epsilon^\alpha(1) &= (0, \vec{k}_1 \times \vec{k} / |\vec{k}_1 \times \vec{k}|), \\ \epsilon^\alpha(2) &= (0, \vec{k} \times (\vec{k}_1 \times \vec{k}) / |\vec{k} \times (\vec{k}_1 \times \vec{k})|), \\ \epsilon^\alpha(3) &= (|\vec{k}|, E_Z \hat{k}) / M_Z; \end{aligned} \quad (4.2)$$

a calculation of (4.1) for the (representative) case $M_Z = 5 \text{ GeV}/c^2$, $E = 50 \text{ GeV}$, and $g_V = g_A$ (V - A coupling) yields

$$\rho_{ab} = \begin{pmatrix} 0.495 & 0.463i & -0.046i \\ -0.463i & 0.457 & -0.060 \\ 0.046i & -0.060 & 0.051 \end{pmatrix}. \quad (4.3)$$

Thus, in terms of the helicity states

TABLE II. Polarization effects with $|g_V| = |g_A|$. An X indicates that the cross section is down by $O(\mu^2)$.

	$g_V = -g_A$	$g_V = +g_A$
Left-handed μ^-	X	Left-handed Z^0
Right-handed μ^-	Right-handed Z^0	X
Left-handed μ^+	Left-handed Z^0	X
Right-handed μ^+	X	Right-handed Z^0

$$\rho_{--} = \frac{1}{2}(\rho_{11} + \rho_{22} - 2i\rho_{12}), \quad (4.4)$$

$$\rho_{++} = \frac{1}{2}(\rho_{11} + \rho_{22} + 2i\rho_{12}),$$

we see that the Z^0 will be produced in an almost pure left-handed state ($\rho_{--} \approx 1$, $\rho_{++} \approx 0$). This result is generally true, independent of the beam polarization, except in the extreme case where terms proportional to the muon mass cannot be neglected in the total cross section.

Calculations at other energies indicate the same high degree of polarization even for very high energies. The interdependence of the beam polarization, observed Z^0 polarization, and relative sign of g_V and G_A is summarized in Table II.

Using our knowledge of the sharp peaking in energy and angle, and the observation that the cross section is dominated by the region where q^2 is small and the muon propagator of Fig. 1a is large, we can construct an approximate expression for the density matrix. Our procedure (adapted from work by Bell and Veltman²³) goes as follows. We rewrite the matrix element as

$$M_a = \frac{J_\mu(\text{proton})}{q^2} \epsilon_\alpha^*(a) \bar{u}(k_2) \left[\left(\frac{2k_1^\mu}{T_1} + \frac{2k_2^\mu}{T_2} \right) \gamma^\alpha - \frac{\gamma^\alpha \not{q} \gamma^\mu}{T_1} - \frac{\gamma^\mu \not{q} \gamma^\alpha}{T_2} \right] (g_V - g_A \gamma_5) u(k_1). \quad (4.5)$$

We next make several observations from our numerical study of the cross sections:

- (1) q^2 is very small, so that to a good approximation $J_\mu = (M_p, \vec{0})$.
- (2) The Z^0 gets most of the incident energy: $\langle E_k \rangle \approx 0.95 \langle E_1 \rangle$, $\langle E_2 \rangle \approx (\mu/M_Z) \langle E_1 \rangle$.
- (3) $T_1 \approx M_Z^2$, while $T_2 \approx -\mu M_Z$.

Then we have

$$M_a \approx \frac{M_p}{q^2} \bar{u}(k_2) \left[\left(\frac{2E_1}{T_1} + \frac{2E_2}{T_2} \right) \not{\epsilon}^*(a) - \frac{\not{\epsilon}^*(a) \not{q} \gamma^0}{T_1} + \frac{\gamma^0 \not{q} \not{\epsilon}^*(a)}{T_2} \right] (g_V - g_A \gamma_5) u(k_1), \quad \not{\epsilon}^* \equiv \gamma \cdot \epsilon^*. \quad (4.6)$$

Analysis of (4.6) indicates that the first two terms in the brackets cancel to a high degree, while using observation (3) above allows us to neglect the third term with respect to the fourth. Thus we obtain

$$M_a \approx \frac{M_p}{q^2} \bar{u}(k_2) \frac{\gamma^0 \not{q} \not{\epsilon}^*(a)}{T_2} (g_V - g_A \gamma_5) u(k_1). \quad (4.7)$$

Performing the spinor algebra of Eq. (4.7), we

can produce approximate predictions for the density matrix elements:

$$\begin{aligned} \rho_{11} &\approx \rho_{22} \approx \frac{1}{2}, \\ |\rho_{13}| &\approx |\rho_{23}| \approx |\rho_{33}| \approx \frac{M_Z}{E_Z} |\rho_{11}|, \\ \rho_{12} &\approx + \frac{i g_V g_A}{(g_V^2 + g_A^2)}. \end{aligned} \quad (4.8)$$

The small terms are not quoted, because they are at the level of the pieces dropped in the approximation; however, the three large terms suffice to give a qualitative picture of the Z^0 polarization in agreement with our numerical example and useful for estimates of the cases where g_V/g_A is arbitrary.

V. SCALAR PRODUCTION

Primarily for purposes of comparison, we consider the possible production of scalar bosons. If a scalar neutral boson exists (e.g., a Higgs scalar or if we were to observe scalar currents), we might expect it to be produced by the same processes shown in Fig. 1 with $Z^0 \rightarrow \phi^0$:

$$\mu + N \rightarrow \mu + N' + \phi^0. \quad (5.1)$$

The calculation of (5.1) goes through in exactly the same way as the work of Secs. II and III with the appropriate changes in the trace. Typical results are shown in Table III and Figs. 7 and 8 for a scalar coupling $g = g_V$. The total rate for (5.1) is smaller than for the Z^0 case by about a factor of 5, and the angular and energy distributions are qualitatively similar.

Most of the factor of 5 may be understood by a simple qualitative argument as follows. We have already remarked that the diagram of Fig. 1(a) dominates the matrix element by virtue of the role of the muon propagator. Then considering $|M|^2$ as given only by Fig. 1(a), we see

$$\begin{aligned} |M|_{Z^0}^2 &\sim g_{\alpha\beta} |\dots \gamma^\alpha u(k_1) \bar{u}(k_1) \gamma^\beta \dots| \\ &\sim 2 |\dots u(k_1) \bar{u}(k_1) \dots| \\ &\sim 2 |M|_{\phi^0}^2. \end{aligned} \quad (5.2)$$

Thus the squares of the matrix elements differ by a factor of 2. Then taking $g = g_V = g_A$ so that $(g_V^2 + g_A^2) \sim 2g^2$ gives another factor of 2, we predict

$$\sigma_\phi \approx \frac{1}{4} \sigma_{Z^0}. \quad (5.3)$$

Of course, the argument is only good to the extent

TABLE III. Total cross sections for $l + p \rightarrow p + \phi^0 + l$ in units of femtobarns ($1 \text{ fb} = 10^{-39} \text{ cm}^2$).

E_1 (GeV)	M_ϕ (GeV/ c^2)	5	10
50		2.9	...
100		17	...
400		91	24
800		150	62

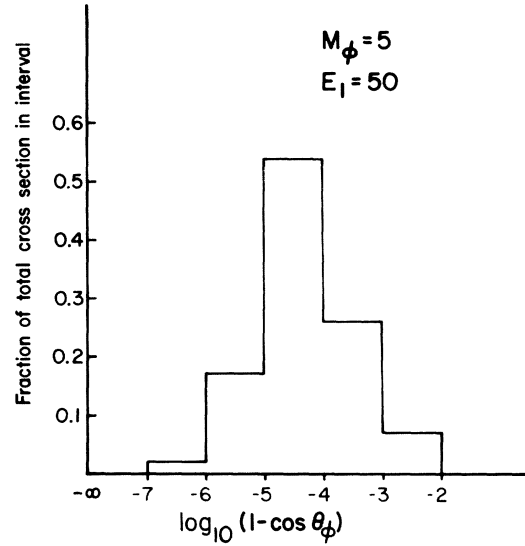


FIG. 7. Histograms of the fraction of the cross section per $\cos\theta_\phi$ interval for free proton targets. Here, $M_\phi = 5 \text{ GeV}/c^2$ and the beam energy is 50 GeV.

that we may ignore the second diagram since the reduction of (5.2) will not work for the cross terms. This may result in an error of about 20% at the energies considered.

VI. DECAY DISTRIBUTION

We restrict our attention here to the leptonic decay mode

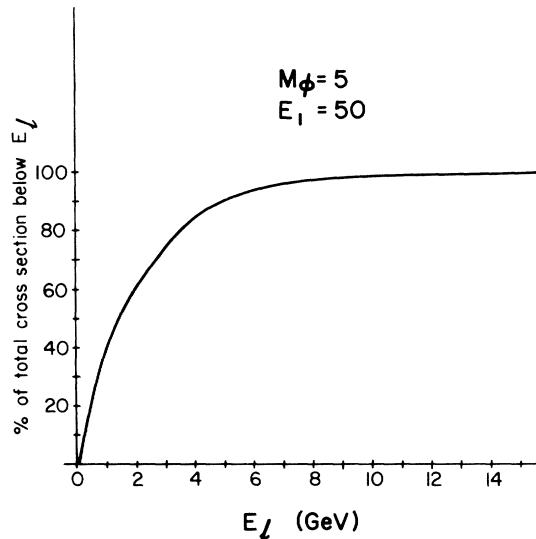


FIG. 8. Plot of the percentage of prompt leptons with energy less than a specific energy E_l for scalar production and free proton targets. The scalar mass and beam energy are as in Fig. 7.

$$Z^0 \rightarrow l^+ + l^-, \quad (6.1)$$

although in fact the hadronic decay modes may be quite important. The questions concerning back-

grounds have pushed us to concentrate on the former.

Working in the rest frame of the Z^0 , one may easily show that the decay distribution is given by

$$\frac{dR_{ab}}{d\Omega^*} = \frac{1}{(2\pi)^3} \frac{1}{4M_Z} \{ (g_V^2 + g_A^2) [k_- \cdot \epsilon(a) k_+ \cdot \epsilon^*(b) + k_- \cdot \epsilon^*(b) k_+ \cdot \epsilon(a) - k_+ \cdot k_- \epsilon(a) \cdot \epsilon^*(b)] - 2i g_V g_A \epsilon_{\alpha\beta\gamma\delta} k_-^\alpha \epsilon^\beta(a) k_+^\gamma \epsilon^{*\delta}(b) \}, \quad (6.2)$$

where k_+ , k_- are the four-momenta of the μ^+ , μ^- , respectively. $d\Omega^*$ is the solid angle in the boson rest frame, and the $\epsilon^\alpha(a)$ are polarization vectors either in terms of the linear polarization basis, Eq. (4.2), or the circular basis,

$$\epsilon(+)=\frac{1}{\sqrt{2}}[\epsilon(1)+i\epsilon(2)],$$

$$\epsilon(-)=\frac{1}{\sqrt{2}}[\epsilon(1)-i\epsilon(2)].$$

Specializing to $g_V = g_A$, and the Z^0 helicity $\lambda = +1$ (-1) for right- (left-) handed Z^0 we get

$$\frac{dR}{d\cos\theta^*} = \frac{g_V^2 M_Z}{16\pi} (1 + \lambda \cos\theta^*)^2. \quad (6.3)$$

It is a simple matter to transform (6.3) to the lab system, since the Z^0 is essentially collinear with the beam, yielding

$$\frac{dR}{d\cos\theta} \cong \frac{g_V^2}{16\pi} \frac{M_Z}{\gamma^3(1-\beta\cos\theta)^2} \left[1 + \lambda \frac{(\cos\theta - \beta)}{1 - \beta\cos\theta} \right]^2, \quad (6.4)$$

$$\gamma = \frac{E_Z}{M_Z}, \quad \beta = \frac{|\vec{P}_Z|}{E_Z}.$$

Making use of the approximations employed in Sec. IV to obtain an expression for the density matrix as a function of g_V and g_A , we can also produce an approximate expression for the average decay distribution:

$$\frac{d\bar{R}}{d\Omega} \cong \text{tr} \left\{ \bar{\rho}_{ab} \frac{dR_{ab}}{d\Omega} \right\}. \quad (6.5)$$

We get

$$\frac{d\bar{R}}{d\Omega} \cong \frac{AM_Z^2}{4} \left[(g_V^2 + g_A^2)(1 + \cos^2\theta^*) - \frac{8g_V^2 g_A^2}{g_V^2 + g_A^2} \cos\theta^* \right], \quad (6.6)$$

where

$$A = \frac{1}{(2\pi)^2} \frac{1}{4\gamma^2 E_Z (1 - \beta \cos\theta)^2},$$

$$\cos\theta^* = \frac{\cos\theta - \beta}{1 - \beta \cos\theta}.$$

Although this result is most reliable for the special case where $g_V = \pm g_A$, it is a fair approximation for other values, and should be useful in understanding how the final decay distribution depends on g_V and g_A . The reader will note that in (6.6) the coefficient of the $\cos\theta^*$ term cannot change sign since this equation summarizes correctly the effect of g_V and g_A for the reaction as a whole. The change in sign of λ is compensated by the change in the sign of g_V/g_A .

VII. DISCUSSION

We must preface these concluding remarks by a caveat. All of our rates have been calculated by the choice $G'_F = G_F$ in Eq. (2.1). Specific models and/or experimental results may well require a change in this coupling strength, but it is a simple matter to scale the numbers in this paper up or down according to the reader's needs. Similarly one may multiply the scalar production cross sections by $\sqrt{2} g^2 / (M_\phi^2 G_F)$, where g is any other preferred scalar coupling, $\mathcal{L}_I = g \bar{\psi} \psi \phi$. In units of e , this coupling is characterized by mass ratios in various gauge theories; in particular, $g = \mu e / (74.6 \text{ GeV})$ in the Weinberg-Salam model²⁵ and $g = e \times (\text{heavy lepton mass}) / M_W$ in the Georgi-Glashow model.²⁶ The former would reduce our cross sections in Table III by at least *three orders of magnitude*.

Our work can be easily generalized to other targets and to inelastic hadron production. That is, the qualitative (and quantitative, modulo simple factors like $\frac{1}{2}$) discussions of these topics in I and II carry right over to our case. In this regard we might mention that the conclusions we have reached about the dependence of the polarization on g_V and g_A are essentially independent of the choice of form factor, and so are equally valid in the general case. Speaking of different choices for form factors, an idea of the uncertainties in our numbers can be found by perusing I and II. We would like to emphasize that the "deep"-inelastic form-factor fit in Eq. (5.9) of I and Eq. (7.4) of II should be updated, but its error is in the right direction since additional contributions in the small invariant

mass region (the region overestimated by our form factor) are needed anyway in order to include resonances.²⁷

As far as a qualitative description of the spectra is concerned, the Z^0 is extremely forward and energetic. This is true for spin-zero as well as spin-one bosons inasmuch as the important determinants are the propagator enhancements and (supposedly) large masses. An important signature then is the order-of-magnitude difference in energy between the "slow" prompt muon and any few-body boson decay products. If the boson decays mainly into hadrons, detection of the prompt muon inclusively would not show a concentration of events at small T and larger energy transfer. The background, virtual-photon excitation of the proton, is too large. An analog of the W -search techniques²⁸ might still be useful in an *exclusive* experiment if additional large transverse momenta cuts are made in the hadron sector. Very likely, the *large-transverse-momentum signature in the boson decay products is the key for these searches.*

The spectrum we have provided for the recoiling proton may be useful in a missing-mass experiment. We have in mind²⁹ the decay mode $Z^0 \rightarrow \nu\bar{\nu}$, which has no counterpart in charged boson studies. (In fact, proton recoil information is absent in I and II although $d\sigma/dT$ curves will yield the average kinetic energy.) Near threshold the proton gets kicked forward and, as the beam energy is increased for a given boson mass, its average scattering angle grows and kinetic energy decreases. For example, Fig. 6 for $M_Z = 5 \text{ GeV}/c^2$ and $E_1 = 50 \text{ GeV}$ shows more than 90% of the events between 8° and 53° and between 80 and 400 MeV kinetic energy for the recoiling proton. These statements are also useful for nuclear targets since incoherent scattering dominates over coherent scattering (unless we are far above threshold).

The ambiguity in g_V and g_A , an issue which is not present for neutrino experiments, has been translated into polarization effects. The use of a polarized lepton beam can determine the relative size and sign of g_V/g_A . (It is interesting that the lepton decay distribution is independent of this relative sign.) By the choices $g_V = e$ and $g_A = 0$, one has the spectra and polarization for heavy

photon production as an added attraction; this augments the total cross section calculations of Linsker.²⁰

What branching ratios do we have a right to expect? The parton model suggests, for lepton-like quark multiplets, that the total decay rate into hadrons should equal the total decay rate into leptons.⁸ Then the $\mu^+\mu^-$ branching ratio would be something like $\frac{1}{8}$. Another approach is to relate the hadronic decay to the colliding beam total hadronic cross section.³⁰ If the ratio $R = \sigma(e^+e^- \rightarrow \text{hadrons}) / (4\pi\alpha^2/3S)$ is bigger at the (large) energy of M_{Z^0} than that predicted in the quark model, we would have a correspondingly smaller $\mu^+\mu^-$ ratio.

Other than to refer to comments in our previous letter⁹ about background and beam polarization expected for μ 's from π decay, we should like to present a final estimate of rates for the production of Z^0 with mass $10 \text{ GeV}/c^2$ and a muon beam energy of 200 GeV. Consider the following Fermilab inputs:

- (1) 1000 h of beam time,
- (2) one million muons per beam pulse,
- (3) one pulse every 6 sec,
- (4) a hydrogen target length of $3000 \text{ g}/\text{cm}^2$.

Adding in our cross section of $2.3 \times 10^{-38} \text{ cm}^2$ for a target proton and a leptonic branching ratio of $\frac{1}{2}$, we get about six leptonic decay events. This suggests that we may have to wait for further experimental progress (especially if the signal-to-noise ratio is a problem) to set a lower limit comparable to that for the charged boson $M_W \gtrsim 10 \text{ GeV}/c^2$.³¹ The Weinberg-Salam gauge theory predicts $M_{Z^0} \gtrsim 74.6 \text{ GeV}/c^2$, and, for that, lower limits will have to satisfy us for some time.

ACKNOWLEDGMENTS

We are most happy to acknowledge the stimulating atmosphere and kind hospitality provided for us by Professor C. N. Yang and the Institute for Theoretical Physics at Stony Brook. Professor Karnig Mikaelian is to be thanked for his participation in the early stages of this study.

APPENDIX A

The phase-space integrations involved here are essentially the same as those detailed in II. The reader can obtain the various integration limits from II if the changes from neutrino to muon kinematics given below are noted.

First, with references to the muon spectra, the following changes should be made (we take $M_Z = 1$):

- (1) The cross-section expressions are to be multiplied by $\frac{1}{2}$ for unpolarized muon beams.

(2) Replace E_1 by $|\vec{k}_1|$ whenever it appears in *denominators*.

(3) In place of Eq. (3.8) in II, use

$$E_2^\pm(\theta) = \frac{1}{2(S + |\vec{k}_1|^2 \sin^2 \theta)} \{ (M_p + E_1)[S + \mu^2 - (M_p + 1)^2] \pm |\vec{k}_1| \cos \theta [(S + \mu^2 - (M_p + 1)^2)^2 - 4\mu^2(S + |\vec{k}_1|^2 \sin^2 \theta)]^{1/2} \}. \quad (\text{A1})$$

(4) In place of Eq. (3.5) in II, use (A1) at $\theta=0$ and

$$S_\mu = S_{\text{th}} + \frac{\mu}{M_p - \mu} (1 + 2\mu). \quad (\text{A2})$$

Second, with reference to the Z^0 spectra, the changes are as follows:

(1), (2) See the muon spectra changes.

(3) In place of Eq. (4.6) in II, use

$$E_k(\theta)_{\text{min}} = \frac{1}{2(S + |\vec{k}_1|^2 \sin^2 \theta)} \{ (M_p + E_1)[S + 1 - (M_p + \mu)^2] \pm |\vec{k}_1| \cos \theta [(S + 1 - (M_p + \mu)^2)^2 - 4(S + |\vec{k}_1|^2 \sin^2 \theta)]^{1/2} \}. \quad (\text{A3})$$

(4) In place of Eq. (4.4) in II, use (A3) at $\theta=0$.

APPENDIX B

This Appendix contains the details of the procedure outlined in Sec. III. In terms of the quantities K and L defined in Eq. (3.4), we can write t_1 and t_2 of Eq. (3.3) as

$$t_2 = \frac{1}{2[q^2 \mu^2 - (k_1 \cdot q)^2]} \left[\frac{3q^2}{q^2 \mu^2 - (k_1 \cdot q)^2} K - L \right], \quad (\text{B1})$$

$$t_1 = \frac{1}{3q^2} \{ L - [q^2 \mu^2 + 2(k_1 \cdot q)^2] t_2 \}.$$

Then, in

$$\sigma = \frac{1}{128\pi^3} \frac{\alpha^2}{|\vec{k}_1| M_p} I, \quad (\text{B2})$$

where

$$I \equiv 2\pi \int |\vec{p}'| dE_{p'} d\cos\theta_{p'} T^{-2} P_{\mu\nu} L^{\mu\nu},$$

it is convenient to change variables to

$$T \equiv q^2 = 2M_p^2 - 2M_p E_{p'} \quad (\text{B3})$$

and

$$S' \equiv (k + k_2)^2 = T - 2k_1 \cdot q + \mu^2.$$

We center our attention, therefore, on the inte-

gral

$$I = \frac{2\pi}{4M_p |\vec{k}_1|} \int_{|T|_{\text{min}}}^{|T|_{\text{max}}} \int_{S'_{\text{min}}}^{S'_{\text{max}}} d|T| dS' T^{-2} P_{\mu\nu} L^{\mu\nu} \quad (\text{B4})$$

in which

$$S'_{\text{min}} = (M_Z + \mu)^2,$$

$$S'_{\text{max}} = 2|\vec{k}_1| |\vec{p}'| + T \left(1 + \frac{E_1}{M_p} \right) + \mu^2,$$

$$|\vec{p}'| = \left(\frac{T^2}{4M_p} - T \right)^{1/2},$$

and

$$|T|_{\text{max}} = \frac{b + (b^2 - 4ac)^{1/2}}{2a},$$

$$|T|_{\text{min}} = \frac{b - (b^2 - 4ac)^{1/2}}{2a}, \quad (\text{B5})$$

with

$$a = S/M_p^2,$$

$$b = 4|\vec{k}_1|^2 - 2(S'_{\text{min}} - \mu^2) \left(1 + \frac{E_1}{M_p} \right), \quad (\text{B6})$$

$$c = (S'_{\text{min}} - \mu^2)^2.$$

Finally,

$$I = \frac{2\pi}{4M_p |\vec{k}_1|} \int \int d|T| dS' S'^{-1} T^{-2} [(S' - M_Z^2 - \mu^2)^2 - 4\mu^2 M_Z^2]^{1/2} \times (A[3T^2 t_1 + T[\mu^2 T + 2(k_1 \cdot q)^2] t_2] + B[T(4M_p^2 - T)t_1 + 4[TM_p^2 E_1^2 + TM_p E_1 k_1 \cdot q + M_p^2 (k_1 \cdot q)^2] t_2]) \quad (\text{B7})$$

using (B1), (3.3), and (2.7), where

$$A \equiv G_M^2,$$

$$B \equiv \frac{G_E^2 + \tau G_M^2}{1 + \tau}.$$

All that now remains is to find K and L . The

integrations corresponding to those in Eq. (3.1) can be analytically in the special frame where $\vec{k}_1 = \vec{q}$ so that $\vec{k}_2 = -\vec{k}$. The calculation is straightforward; the cumbersome resulting expressions will not be given here, but rather left for private communication.

*Work supported in part by the National Science Foundation under Grant No. GP-32998X.

†On leave from Case Western Reserve University, Cleveland, Ohio 44106. Work supported in part by the National Science Foundation under Grant No. GP-33119.

¹F. J. Hasert *et al.*, Phys. Lett. 46B, 121 and 138 (1973); A. Benvenuti *et al.*, Phys. Rev. Lett. 32, 800 (1974); B. Aubert *et al.*, *ibid.* 32, 1454 and 1457 (1974); P. Schreiner, in *Proceedings of the XVII International Conference on High Energy Physics*, edited by J. R. Smith (Rutherford Laboratory, Chilton, Didcot, Berkshire, England, 1974), p. IV-123.

²See, for example, E. S. Abers and B. W. Lee, Phys. Rep. 9C, 1 (1973).

³N. Cabibbo and R. Gatto, Phys. Rev. 124, 1577 (1961).

⁴H. R. Reiss and V. Wataghin, Phys. Rev. 136, B214 (1964).

⁵J. R. Primack and H. Quinn, Phys. Rev. D 6, 3171 (1972). This reference concentrates on Higgs scalar production inasmuch as the Z^0 is presumed to be so massive. For virtual effects in colliding beams, see J. Godine and A. Hankey, Phys. Rev. D 6, 3301 (1972); A. Love, Lett. Nuovo Cimento 5, 113 (1972); V. K. Chung, A. K. Mann, and E. A. Paschos, Phys. Lett. 41B, 355 (1972).

⁶J.-E. Augustin *et al.*, Phys. Rev. Lett. 33, 1406 (1974).

⁷J. J. Aubert *et al.*, Phys. Rev. Lett. 33, 1404 (1974).

⁸R. L. Jaffe and J. R. Primack, Nucl. Phys. B61, 317 (1973).

⁹R. W. Brown, L. B. Gordon, and K. O. Mikaelian, Phys. Rev. Lett. 33, 1119 (1974).

¹⁰See, for example, the analogous charged weak boson calculations by H. W. Fearing, M. Pratap, and J. Smith, Phys. Rev. D 5, 158 (1972).

¹¹For an application to $J(\psi)$ production, see A. De Rújula and S. L. Glashow, Phys. Rev. Lett. 34, 46 (1975). Equation (11) of this reference has an obvious misprint.

¹²R. W. Brown, L. B. Gordon, J. Smith, and K. O. Mikaelian, State University of New York at Stony Brook Report No. ITP-SB-75-20, 1975 (unpublished).

¹³A preliminary estimate for this neutrino reaction can be found in Ref. 9.

¹⁴Compare the estimates of (i) and (ii) in Ref. 9.

¹⁵For example, the proposed ISABELLE facility at Brookhaven.

¹⁶Metric conventions etc. follow those used in J. D. Bjorken and S. D. Drell, *Relativistic Quantum Mechanics* (McGraw-Hill, New York, 1964); *Relativistic Quantum Fields* (McGraw-Hill, New York, 1965).

¹⁷For the record, the triangle anomaly does not enter in lowest order.

¹⁸The fact that muon mass terms enter only on the 1% level has been checked by explicit calculation.

¹⁹R. W. Brown and J. Smith, Phys. Rev. D 3, 207 (1971); R. W. Brown, R. H. Hobbs, and J. Smith, *ibid.* 4, 794 (1971). (These are hereafter referred to as I and II, respectively.)

²⁰Notice that our numbers compare well, when the coupling is suitably modified, with the heavy photon total cross sections calculated by R. Linsker, Phys. Rev. Lett. 27, 167 (1971); Phys. Rev. D 5, 1709 (1972).

²¹We merely tack the spin average factor onto the leading-logarithm expression for W^+ production by neutrinos found in H. Überall, Phys. Rev. 133, B444 (1965).

²²The Cottingham decomposition [W. N. Cottingham, Ann. Phys. (N.Y.) 25, 424 (1963)] has been used in earlier charged boson production computation by G. von Gehlen, Nuovo Cimento 30, 859 (1963).

²³See II or J. S. Bell and M. Veltman, Phys. Lett. 5, 151 (1963).

²⁴H. Strubbe, Comp. Phys. Comm. 8, 1 (1974).

²⁵S. Weinberg, Phys. Rev. Lett. 19, 1264 (1967); 27, 1688 (1971); A. Salam, in *Elementary Particle Theory: Relativistic Groups and Analyticity* (Nobel Symposium No. 8), edited by N. Svartholm (Almqvist and Wiksell, Stockholm, 1968), p. 367.

²⁶See the $O(3)$ version discussed in J. D. Bjorken, C. H. Llewellyn Smith, Phys. Rev. D 7, 887 (1973).

²⁷Our phenomenological fit is compared with vector dominance in V. V. Makeev *et al.*, Yad. Fiz. 16, 546 (1972) [Sov. J. Nucl. Phys. 16, 304 (1973)]. It is seen that, indeed, our fit gives larger cross sections, a difference which would be reduced if resonance contributions were added in to these other calculations. [See H. H. Chen, Nuovo Cimento 69A, 585 (1970) in which the $N^*(1236)$ channel has been considered.]

²⁸D. Cline, A. K. Mann, and C. Rubbia, Phys. Rev. Lett. 25, 1309 (1970).

²⁹Interest in this decay mode arose when the $J(\psi)$ particles were construed as weak boson production. We thank Professor S. Wojcicki for communicating this interest.

³⁰L.-F. Li and E. A. Paschos, Phys. Rev. D 3, 1178 (1971); C. Jarlskog, Proc. of the 1974 CERN School of Physics, p. 1.

³¹D. Cline, in *Neutrinos-1974*, Proceedings of the Fourth International Conference on Neutrino Physics and Astrophysics, Philadelphia, edited by C. Baltay (A.I.P., New York, 1974), p. 201.